

Inertial Confinement Fusion with Tetrahedral Hohlräume at OMEGA

J. M. Wallace, T. J. Murphy, N. D. Delamater, K. A. Klare, J. A. Oertel, G. R. Magelssen,
E. L. Lindman, A. A. Hauer, and P. Gobby

Los Alamos National Laboratory, Los Alamos, New Mexico 87545

J. D. Schnittman, R. S. Craxton, W. Seka, R. Kremens, and D. Bradley

Laboratory for Laser Energetics, University of Rochester, Rochester, New York 14623-1299

S. M. Pollaine, R. E. Turner, and O. L. Landen

Lawrence Livermore National Laboratory, Livermore, California 94551

D. Drake

InterScience, Germantown, Maryland 20875-0659

J. J. MacFarlane

University of Wisconsin, Madison, Wisconsin 53706

(Received 2 November 1998)

Indirect-drive inertial confinement fusion will require for ignition a highly symmetric x-ray flux around the capsule. To this end, the “tetrahedral hohlraum,” spherical in shape with four laser entrance holes located at the vertices of a tetrahedron, has been proposed. The first experimental test of this concept, using the OMEGA laser, is reported here. Drive symmetry was probed using capsule implosion symmetries, which varied qualitatively as expected with hohlraum dimensions. Modeling of the experiments gives time-averaged flux asymmetries as low as 1% rms over a 2.2-ns laser pulse. [S0031-9007(99)09118-8]

PACS numbers: 52.40.Nk, 52.50.Jm, 52.58.Ns

Inertial confinement fusion requires for its efficient implementation a highly symmetric capsule implosion. With the indirect-drive approach, this in turn requires a highly symmetric thermal x-ray drive flux around the capsule [1]. Using a laser driver, this is achieved by directing clusters of beams onto the inside wall of a high- Z radiation case, or hohlraum, which symmetrizes the flux by the continual absorption and reemission of soft x-ray radiation over the entire wall area [2]. Recently, the concept of the “tetrahedral hohlraum,” which is a spherical radiation case with four laser entrance holes (LEHs) located at the vertices of a tetrahedron, has been proposed as an effective means for achieving highly symmetric radiation drive [3,4]. This is an alternative to the cylindrical hohlraum with two LEHs located on the ends, which has been employed in most hohlraum experiments performed to date [5,6]. It bears some resemblance, however, to the 6-LEH, spherical hohlraums fielded at the Iskra-5 laser with 12 beams, for which a high degree of capsule irradiation uniformity has been reported [7].

This Letter reports the first test of the tetrahedral concept, which was performed at the 60-beam, upgraded OMEGA laser [8]. The drive symmetry was diagnosed from x-ray self-emission images of imploded capsule cores [9,10]. The capsule-implosion symmetry varied qualitatively as expected with hohlraum dimensions, scaling with the time-averaged rms flux asymmetry on the capsule, $\langle A_{\text{rms}} \rangle$, calculated with view-factor codes [4,11]. An $\langle A_{\text{rms}} \rangle$ as low as 1% over a 2.2-ns laser pulse is given by

the modeling for conditions of the most symmetric implosions, which gave x-ray images round to within (4–8)%. The basic energetics of the hohlraums and the capsule neutron yields agreed with one-dimensional (1D) simulations using the radiation-hydrodynamics code LASNEX [12].

A schematic of the tetrahedral hohlraum, produced by a three-dimensional visualization code [13], which shows the individual beam cones entering one of the LEHs and the centrally located fusion capsule, is given in Fig. 1. The 60-beam configuration, like the hohlraum itself, has tetrahedral symmetry [14] with 15 beams introduced at each of the four LEHs. These 15 incoming beams are subdivided into five groups of three beams, each group having threefold rotation symmetry about an axis extending from target center through the LEH center. The beam centroids of each group define a cone, having cone angle 23.2° (2 cones), 48.8° (2 cones), or 58.8° (1 cone) with respect to the axis specified above. Beam pointing is strongly constrained: Each beam must clear the edge of the LEH where it enters, avoid the capsule in its initial, unimploded configuration, avoid exiting the hohlraum through an LEH on an opposite wall, and have a maximum intensity at the wall of $\sim 10^{15}$ W/cm². The rms deviation from the mean of the 60 beam energies varied from shot to shot in the range (5–17)%, but was typically $\sim 12\%$. The rms beam pointing accuracy at the hohlraum wall was ~ 30 μm .

Two different size hohlraums were employed, having inside radii $r_h = 1150$ and 1400 μm . The LEH radii were $r_{\text{LEH}} = 450$ μm for the smaller targets and 350, 450, or



FIG. 1(color). Schematic of the tetrahedral hohlraum. The 15 laser beams entering one of the LEHs are indicated by the cones, which show the beam footprints on the front-side hohlraum wall. In this view two of the four LEHs, indicated by the spoked-wheel patterns, are seen on the front. The LEHs on the rear side are indicated by solid coloring. The capsule is shown at the center of the target in its initial configuration. This image was produced by the three-dimensional visualization code used in the design of the targets.

500 μm for the larger targets. (A hohlraum of radius r_h and LEH radius r_{LEH} will be designated by r_h/r_{LEH} .) The targets were thin-wall [15], vacuum hohlraums, fabricated of Au having thickness 2 μm , surrounded by an outer support layer of epoxy 100 μm thick, machined down to a 25 μm thickness in the vicinity of the LEHs to avoid beam clipping. The capsules were identical to designs previously fielded on NOVA [5,9,10]. They had an inside diameter of 440 μm , a plastic shell thickness of 55 μm , and deuterium fill pressure of 50 atm doped with 0.1 atm of Ar for imaging purposes. The capsules were mounted at the center of the hohlraum using a Formvar web.

The capsule core images were obtained with time-integrated pinhole cameras (magnification $4\times$) and gated x-ray framing cameras (magnification $12\times$) with ~ 50 ps time resolution. Both employed 5 μm pinholes, which provide adequate spatial resolution for the 50- μm -diam core images. Images were viewed through the wall with transmitted 4–8 keV photons and through the LEHs with 2–8 keV photons.

To establish contact with previous hohlraum experiments performed on the NOVA and OMEGA lasers [5,9,16], the experiments used two different laser temporal pulse shapes for which large databases exist: a 1-ns flattop and a 2.2-ns shaped pulse with a 1-to-3 intensity contrast ratio between a leading 1-ns foot and the main pulse. The total energy delivered to the target in $\lambda = 0.35$ μm laser light was typically 31–33 kJ for the 1-ns pulse and 21–

25 kJ for the shaped pulse. The overall energetics of the tetrahedral hohlraum were investigated in the absence of a capsule. The thermal radiation temperature was measured using the Dante diagnostic [17], viewing through one of the LEHs. The Dante field of view includes a mix of irradiated and unirradiated wall area and LEH area similar to what the capsule would see. Consequently, no “albedo corrections” [18] to the data were made. The stimulated Brillouin scatter (SBS) in the backward direction was measured on one beam in a 48.8° cone and was seen to have time dependence similar to the laser pulse shape. The time-integrated backscatter fraction ranged from (3–15)% of the beam energy, depending on the target parameters, in general agreement with measurements on comparable cylindrical vacuum hohlraums [19]. Observations on beams with the other two cone angles will be required for a more precise determination of the total backscatter fraction. Figure 2 shows a comparison between the radiation temperature determined by Dante and the corresponding 1D LASNEX simulation. The simulation employed the observed pulse shape (shaped pulse) in an internally sourced laser beam. It accounted for SBS backscatter by an overall reduction in the total laser energy on target by the backscatter fraction observed on the one beam. The non-local-thermodynamic-equilibrium atomic physics package [12] was used for a proper treatment of the laser-plasma interaction at the Au wall. The LEH radiation losses were incorporated using a σT_R^4 model applied to the known total hole area. The agreement between observation and simulation is satisfactory, with a maximum temperature inferred from Dante of 180 eV. Comparable agreement, generally within the accuracy of the diagnostic ($\sim 5\%$), was obtained for the complete range of targets

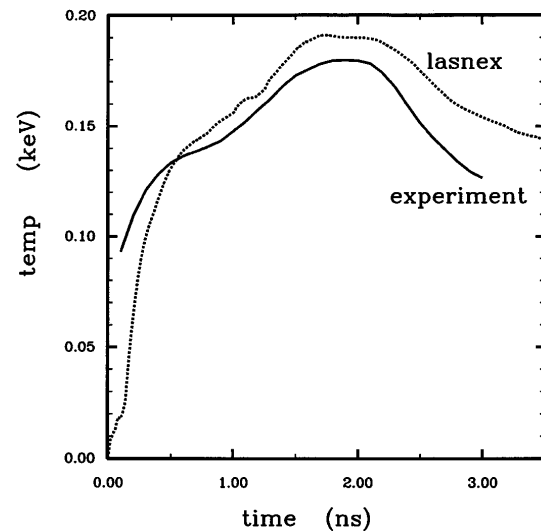


FIG. 2. Radiation temperature versus time for a 1400/500 tetrahedral hohlraum which contains no capsule. The shaped laser pulse, with a total energy on target of 22 kJ, was used. The SBS backscatter fraction was 6%. The solid curve is the Dante result and the dotted curve is the corresponding 1D LASNEX result.

shot. (The 3D view-factor code BUTTERCUP [4], which employs a 1D radiation diffusion treatment at each point on the hohlraum wall but omits hydrodynamic motion, gives radiation temperatures which agree closely with the LASNEX results.) The results for all the empty-hohlraum shots, including the maximum radiation temperature, the ratio of observed to calculated maximum temperature, and the SBS backscatter fraction, are given in Table I. The highest maximum radiation temperature 229 eV was obtained with the smaller hohlraum and the 1-ns pulse. The same computational procedure was employed to simulate hohlraums containing capsules, assuming no mix across the gas-pusher interface. The capsule convergence ratios are given to be $C_r \cong 10$ ($C_r \equiv$ initial capsule ablator radius/fuel radius at maximum neutron emission). Neutron yields from simulation and observation could be brought into agreement for the better performing capsules by modest reductions in the hohlraum radiation temperature in LASNEX within the range of uncertainty in the Dante data.

Considering now the radiation flux symmetry, Fig. 3 presents computational predictions for the asymmetry on the capsule together with the observed capsule core images for two substantially different hohlraums. The results on the left are for an 1150/450 hohlraum with a 1-ns pulse; the results on the right are for a more symmetrical 1400/350 hohlraum with the shaped pulse. The upper plots are view-factor calculations [11] of σ_{32} , the Y_{32} component of A_{rms} [14] obtained using the time-dependent wall albedos, $\alpha(t)$, from the 1D LASNEX simulations. The calculations show that A_{rms} is produced predominately by σ_{32} as in Ref. [4]. This is consistent with Ref. [3], which shows that the $l = 3, 4$ components are the lowest-order, nonvanishing contributions to the flux asymmetry for an ideal tetrahedral target. The predicted asymmetry was reduced in the right-hand target by increasing r_h , i.e., increasing the case-to-capsule area ratio, and decreasing r_{LEH} , diminishing the effects of the cold holes. The core self-emission images, shown in the lower portion of Fig. 3, reflect the flux asymmetries experienced by the capsules during their implosions. These images were taken along a line of sight through an LEH or through the thin wall directly opposite an LEH. Images obtained in these two directions were usually in good agreement. The distortion

d of the image from sphericity, which is extracted from the 50% intensity contour, will be used as a quantitative measure of the implosion symmetry. Specifically it is the ratio of the maximum to minimum (minimum to maximum) radius of the $m = 3$ Fourier component of the 50% contour when the image lobes point generally toward (midway between) the opposite three LEHs [20]. For the triangular, left-hand image, the lobes point toward the opposite three LEHs, which are predicted to be “cold spots” in the flux distribution where the drive is minimum and the capsule convergence would be locally reduced, as observed. In this case $d = 1.16$. The core image on the right is significantly more symmetrical with $d = 0.96$, consistent with the reduction in σ_{32} given by the view-factor calculation. The result $d < 1$ indicates a hole-hot average flux asymmetry, although the effect is quite small. For this implosion, the calculated T_R^4 -weighted, time-averaged asymmetry is $\langle A_{\text{rms}} \rangle \sim 1\%$, a factor-of-3 reduction from the left-hand case. The observed implosion symmetry correlates with the predicted flux asymmetry. The correlation is supported by 3D implosion simulations with prescribed tetrahedral flux asymmetry and the simplified atomic and radiation physics models currently available in 3D [21]. The overall drive-symmetry picture should become clarified with the development of fully integrated 3D radiation-hydrodynamics simulation capability, which will make possible a more reliable determination of A_{rms} from capsule-implosion data. Prior to the shots there was concern for the 58.8° beams, which skirt the ablating Au wall for an extended distance, and for the 23.2° beams, which are focused inside the hohlraum in the path of the capsule blowoff. This could have caused undesired beam deflection, enhanced SBS, or possibly other undesired effects. There was, however, no evidence of target degradation from these phenomena, possibly because the target ideally retains tetrahedral symmetry, with the suppression of $l = 1, 2$ components, regardless of 3D effects.

To summarize, the concept of the tetrahedral hohlraum has been tested for the first time in a series of shots using the 60-beam OMEGA laser. For a range of hohlraum parameters and two different laser-intensity pulse shapes, the overall energetics of the hohlraum and capsule neutron yields were in general agreement with 1D simulations using the LASNEX code. A maximum radiation temperature

TABLE I. Empty-hohlraum radiation temperatures.

Hohlraum r_h/r_{LEH}	Pulse shape	Laser energy (kJ)	$(T_R)_{\text{Dante}}$ (eV)	Observed/ calculated	SBS backscatter
1150/450	Flattop	31.5	219	0.96	N.A.
1150/450	Flattop	31.0	229	1.01	5.4%
1150/450	Shaped	25.1	198	0.96	9.5
1400/450	Flattop	32.0	209	0.95	3.4
1400/500	Shaped	22.0	180	0.94	7.1
1400/350	Shaped	21.7	189	0.94	4.8
1400/350	Shaped	22.1	180	0.95	14.8
CH lined					

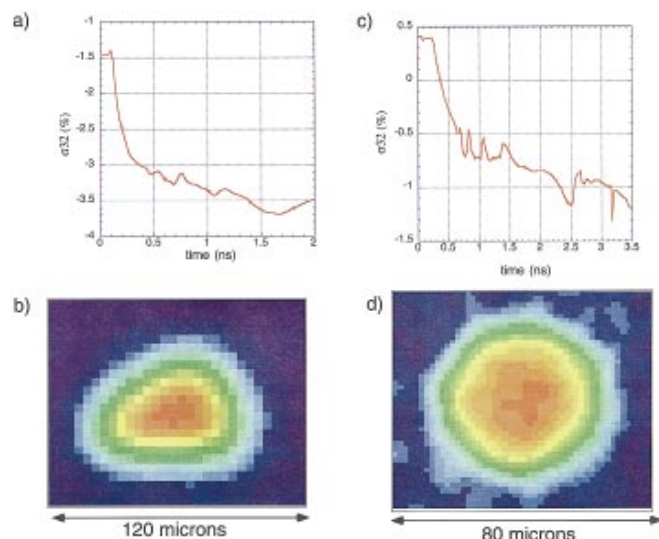


FIG. 3(color). Comparison between two different tetrahedral-hohlraum designs: the 1150/450 target with the 1-ns pulse on the left and the 1400/350 target with the shaped pulse on the right. Plots (a) and (c) show σ_{32} , the predicted time-dependent rms flux-asymmetry component. $\sigma_{32} < (>) 0$ indicates a hole-cold (hole-hot) configuration. The lower part of the figure shows the corresponding x-ray images for the two capsule implosions. Image (b), obtained with the smaller hohlraum, shows a triangular pattern having $d = 1.16$ with the lobes pointing toward the three opposite LEHs (not shown). Image (d), obtained with the larger hohlraum, is more nearly round, $d = 0.96$, and is consistent with the more symmetrical flux distribution predicted by the view-factor calculations.

of 230 eV was observed with the 1-ns laser pulse. The x-ray images of the most symmetric implosions, which had predicted convergence ratio $C_r = 10$, were spherical to within (4–8)%, showing that the tetrahedral hohlraum is indeed capable of producing very spherical implosions. The modeling for these implosions gives an average rms flux asymmetry in the 1% range. In other shots, where the implosion asymmetry could be clearly resolved, the qualitative features of a dominant Y_{32} component were observed, as expected from basic symmetry considerations. The implosion symmetry could be controlled by the systematic variation of hohlraum dimensions and scaled in a manner consistent with the predicted capsule flux asymmetry. A full assessment of the tetrahedral hohlraum for advanced laser drivers will require consideration of gas fill, beam smoothing, beam bending and stimulated scattering processes under relevant plasma conditions, and possibly other features of ignition hohlraums now under consideration [1,19].

The authors thank the OMEGA operations crew and the target-fabrication groups at Los Alamos and Livermore, whose efforts were crucial to the success of this work. This work was performed under the auspices of the U.S. Department of Energy by Los Alamos National Laboratory under Contract No. W-7405-Eng-36, by the Laboratory for Laser Energetics under Cooperative Agreement

No. DE-FC03-92SF19460, and by Lawrence Livermore National Laboratory under Contract No. W-7405-Eng-48.

- [1] J. Lindl, *Phys. Plasmas* **2**, 3933 (1995).
- [2] M. Murakami and K. Nishihara, *Jpn. J. Appl. Phys.* **25**, 242 (1986); A. Caruso, in *Inertial Confinement Fusion, Proceedings Course and Workshop, Varenna, 1988* (Casa Editrice Compositori, Bologna, 1988), p. 139; M. Murakami and J. Meyer-Ter-Vehn, *Nucl. Fusion* **31**, 1315 (1991); **31**, 1333 (1991).
- [3] D. W. Phillion and S. M. Pollaine, *Phys. Plasmas* **1**, 2963 (1994).
- [4] J. D. Schnittman and R. S. Craxton, *Phys. Plasmas* **3**, 3786 (1996).
- [5] L. J. Suter *et al.*, *Phys. Rev. Lett.* **73**, 2328 (1994); *Phys. Plasmas* **3**, 2057 (1996).
- [6] T. J. Murphy *et al.*, *Phys. Plasmas* **5**, 1960 (1998).
- [7] S. A. Bel'kov *et al.*, *JETP Lett.* **67**, 171 (1998).
- [8] T. R. Boehly *et al.*, *Opt. Commun.* **133**, 495 (1997).
- [9] A. A. Hauer *et al.*, *Phys. Plasmas* **2**, 2488 (1995).
- [10] A. A. Hauer *et al.*, *Rev. Sci. Instrum.* **66**, 672 (1995).
- [11] D. Drake, *J. Comput. Phys.* **87**, 73 (1990); J. J. MacFarlane, *Bull. Am. Phys. Soc.* **42**, 2009 (1997).
- [12] G. Zimmerman and W. Kruer, *Comments Plasma Phys.* **11**, 51 (1975); W. A. Lokke and W. Grasberger, LLNL Report No. UCRL-52276, 1977; G. Pollak, LANL Report No. LAUR-90-2423, 1990.
- [13] K. A. Klare, J. M. Wallace, and D. Drake, *Bull. Am. Phys. Soc.* **42**, 1993 (1997).
- [14] For the analysis, a Cartesian coordinate system is employed where the four LEHs are centered along the vectors $(1, -1, -1)/\sqrt{3}$, $(-1, 1, -1)/\sqrt{3}$, $(-1, -1, 1)/\sqrt{3}$, and $(1, 1, 1)/\sqrt{3}$. Tetrahedral symmetry then means that the system (the hohlraum target and the beams) is invariant under cyclic permutations of x, y, z coordinates and under the sign change of pairs of coordinates. In formal mathematical terms, the system is invariant under the 12 rotation operators which constitute the tetrahedral group T ; cf. M. Hamermesh, *Group Theory and its Application to Physical Problems* (Addison-Wesley, Reading, MA, 1962), p. 48ff. The spherical harmonic expansion of the radiation flux is taken in this system.
- [15] D. A. Baker, K. A. Klare, J. A. Oertel, J. M. Wallace, R. G. Watt, J. M. Murray, and M. C. Rushford, *Bull. Am. Phys. Soc.* **38**, 2083 (1993); J. M. Wallace, D. A. Baker, N. D. Delamater, E. L. Lindman, and J. A. Phillips, *Bull. Am. Phys. Soc.* **39**, 1685 (1994); D. A. Baker, J. M. Wallace, G. D. Craig, A. A. Hauer, J. M. Murray, J. A. Oertel, and R. G. Watt, *Def. Res. Rev.* **6**, 13 (1994); N. D. Delamater *et al.*, *Phys. Plasmas* **3**, 2022 (1996).
- [16] T. J. Murphy *et al.*, *Phys. Rev. Lett.* **81**, 108 (1998).
- [17] H. N. Kornblum, R. L. Kauffman, and J. A. Smith, *Rev. Sci. Instrum.* **57**, 2101 (1986); R. L. Kauffman *et al.*, *Phys. Rev. Lett.* **73**, 2320 (1994).
- [18] C. Decker *et al.*, *Phys. Rev. Lett.* **79**, 1491 (1997).
- [19] R. L. Kauffman *et al.*, *Phys. Plasmas* **5**, 1927 (1998).
- [20] T. J. Murphy *et al.*, *Bull. Am. Phys. Soc.* **43**, 1902 (1998).
- [21] S. Pollaine, M. Marinak, and D. Munro, *Bull. Am. Phys. Soc.* **42**, 1993 (1997).